Eur. Phys. J. A **22**, 271–275 (2004)
DOI 10.1140/epja/i2004-10016-x

THE EUROPEAN PHYSICAL JOURNAL A

Fission barriers of super-heavy nuclei produced in cold-fusion reactions

J. Péter[a]

LPC Caen - ENSICAEN 6, boulevard du Maréchal Juin, 14050 Caen cedex, France

Received: 29 January 2004 / Revised version: 29 March 2004 /
Published online: 9 November 2004 –
Communicated by D. Guerreau

Abstract. Excitation functions of super-heavy evaporation residues formed in cold-fusion reactions were analyzed with the aim of getting information on the fission barrier height of these nuclei. The method uses the location of the maximum of 1n and 2n excitation functions. The results obtained on nuclei from $Z = 104$ to 112 are compared to three theoretical predictions.

PACS. 25.70.Jj Fusion and fusion-fission reactions – 24.75.+i General properties of fission

1 Introduction

The fission barrier height is a fundamental characteristics of a super-heavy nucleus, since the existence of a fission barrier is the condition for the formation of such a compound nucleus. It has a practical importance for the possibility to produce evaporation residues (ERs), since it governs the survival probability of the compound nucleus and therefore the very small cross-sections of ERs ($<$ 1 pb for elements above 112). It also governs the spontaneous-fission lifetime of these ERs, with two consequences: i) when this lifetime becomes similar to the ER time-of-flight from the target to the implantation detector, the detection efficiency of the ERs is strongly reduced (eventually to the point of becoming negligible); ii) when the fission lifetime becomes shorter than the α-decay lifetime, fission occurs preferentially; the present techniques do not allow to obtain the A and Z values of the two fission fragments and to reconstruct the fissioning nucleus; therefore this detection does not provide an identification as clear as the observation of a chain of α-particles ending on a known isotope. A good estimate of Bf is mandatory for predicting the cross-section, lifetime and radioactive decay of new elements or isotopes. Any experimental information is of much interest.

The excitation functions of residual nuclei formed at Dubna in hot-fusion reactions were used in cases where the compound-nucleus cross-sections had been experimentally measured [1]. The survival probability was calculated using usual statistical formulas. By fitting the calculated xn excitation functions to the experimental ones, lower limits of fission barrier heights were obtained for several isotopes of elements 112, 114 and 116 [2].

In this paper, we are interested in other isotopes, formed at smaller excitation energies, and the fission barrier heights were extracted using another method.

An attempt is made to extract the fission barrier of isotopes formed at GSI and RIKEN in cold-fusion reactions with ^{208}Pb or ^{209}Bi target nuclei [3,4]. Figure 1 shows the values predicted by three different macroscopic-microscopic approaches for compound nuclei with $Z = 104$ to 114 formed in these reactions and for the 1 neutron and 2 neutrons evaporation residues. The table of Moeller *et al.* [5] gives the shell correction to the potential energy at ground state; the macroscopic barrier (liquid drop) at the saddle was added by Aritomo [6] and varies from 0.8 MeV to 0 for the nuclei under consideration (Note: a convenient formula is given by Swiatecki *et al.* in [7]). Similar values are given in [8]. Mamdouh *et al.* [9] used the extended Thomas-Fermi plus Strutinsky integral method. In the work of Muntian *et al.* [10] the macroscopic part is based on the Yukawa-plus-exponential model and the Strutinsky correction is based on the Wood-Saxon single-particle potential. Large differences are observed between these predictions, especially when approaching $Z = 114$ which is a possible magic number.

Since the compound nucleus cross-sections are not known experimentally and theoretical calculations differ by orders of magnitude, the method used in [2] (fitting cross-section values) cannot be used here. We rely on the *peak locations* of 1n and 2n excitation functions, $E^*_{\rm max}$(1n) and $E^*_{\rm max}$(2n). Indeed, the center-of-mass incident energy necessary to reach the maximum of the 1n excitation function is given by the sum of the fusion mass balance Q (difference between the projectile and target masses and

[a] e-mail: jpeter@in2p3.fr

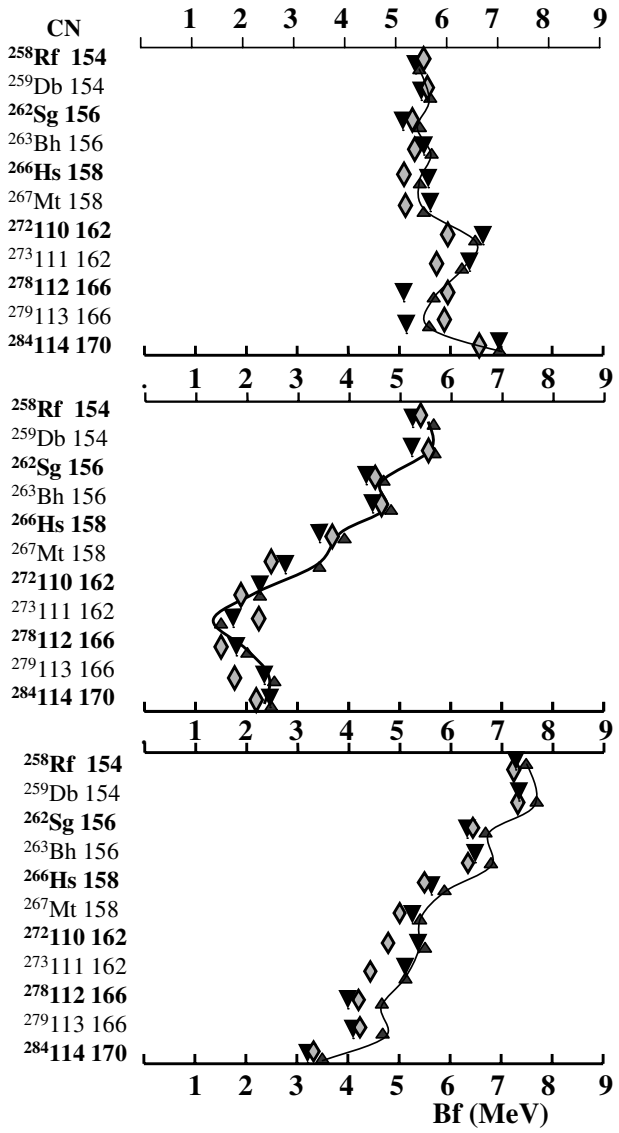

Fig. 1. Theoretical fission barrier values of nuclei formed in cold-fusion reactions with ^{208}Pb or ^{209}Bi according to three tables. Top: Moeller *et al.* [5] plus liquid-drop contribution at saddle. Center: Mamdouh *et al.* [9]. Bottom: Muntian *et al.* [10]. Compound nuclei: downward triangles. Evaporation residues: 1n = upward triangles; 2n = diamonds. The lines connecting 1n values are just to guide the eye.

the compound nucleus mass), the neutron separation energy of the neutron emitted by this compound nucleus and the fission barrier of the residual nucleus plus about 1 MeV [11]. Conversely, the experimental determination of the peak location makes it possible to obtain the fission barrier height, provided the compound nucleus mass and its first neutron separation energy are known. An elegant expression for the energy of the 1n excitation function was given by Swiatecki who uses the mass of the fission saddle-point of the residual nucleus plus the mass of a neutron minus the masses of target and projectile plus about 0.5 MeV [7]. The experimental excitation functions are those of $Z = 104$ to 112 nuclei formed in fusion between ^{208}Pb or ^{209}Bi and projectiles ranging from ^{50}Ti to ^{70}Zn. These compound nuclei have two common features: i) all of them have an even neutron number; ii) the incident energy which corresponds to $E^*_{\rm max}$(1n) is much smaller than the Bass barrier $V_{\rm B}$ (Coulomb barrier) at $Z = 104$ and moves up to $V_{\rm B}$ at $Z \sim 110$; the incident energy for $E^*_{\rm max}$(2n) is slightly smaller or close to $V_{\rm B}$ for $Z = 104$–107 (and was not measured for $Z \geq 108$).

2 Simulated excitation functions

Experimental 1n excitation functions were simulated in three steps as illustrated in fig. 2.

In the first step, only the competition between fission and neutron evaporation is considered: it is described with usual Γn/(Γf + Γn) statistical formulas. It depends on the neutron separation energy and fission barrier of the compound nucleus and the 1n evaporation residues, Sn(CN) and Bf(CN), Sn(CN−1n) and Bf(CN−1n). The level density parameters a_n and a_f do not play any role on $E^*_{\rm max}$(1n) values. Monte Carlo calculations were performed with a large number of events at each excitation energy E^*, in 0.1 MeV bins. The Maxwellian kinetic-energy distribution of evaporated neutrons was taken into account. The left panel exhibits the excitation function of this survival probability. Its maximum is located in the 0.1 MeV bin just above Sn(CN) + [the smallest one of Bf(CN−1n) and Sn(CN−1n)], *i.e.* when second-chance fission or second neutron evaporation becomes energetically possible. Earlier, it was assumed that the average kinetic energy of the first neutron should be added (about 1 MeV [11]), but the present Monte Carlo calculation invalidates this assumption. This shape and location would be the shape and location of the 1n excitation function if the fusion cross-section excitation function would be flat.

Second step: each point of this survival probability must be multiplied by the corresponding fusion cross-section. We are not interested here in the absolute value of the fusion cross-section, but only on its variation with energy. Since this range of energy is well below the Bass barrier, the fusion cross-section decreases exponentially with decreasing energy. More than two orders of magnitude were measured for an energy difference of 5 MeV on the system ^{48}Ca + ^{208}Pb [12]. Theoretical calculations give similar behaviours [13,14]. The resulting excitation function is shown in the center panel. The effect of interest here is a displacement of $E^*_{\rm max}$(1n) to a higher value, DE1: 0.8 MeV in this example.

Third step: in order to compare this shape and $E^*_{\rm max}$(1n) to experimental data, the energy resolution of these data has to be taken into account. The projectile energy decreases through the target thickness. The corresponding excitation energy variation is 2.5 MeV to 3.5 MeV [3,4]. In the shown example, 3 MeV was used and the simulated points are plotted at mid-target energy as for experimental data. They exhibit a Gaussian shape (fig. 2 right), like the data.

The FWHM of these distributions decreases from 3.2 MeV (left) to 2.8 MeV (center) and increases at right

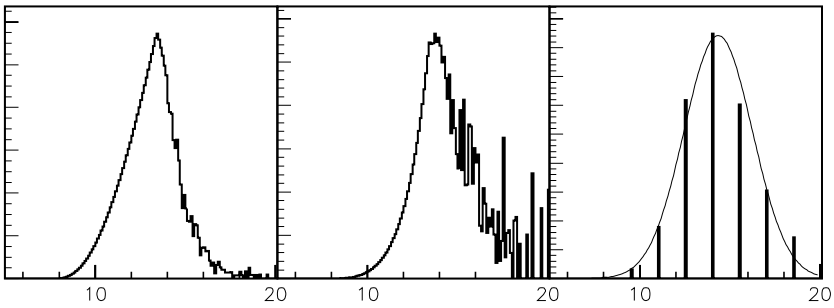

Fig. 2. Simulated 1n excitation functions. Horizontal scale: excitation energy (MeV) in 0.1 MeV bins. Vertical scale: cross-section in arbitrary units, linear scale. Left: survival probability $\Gamma n/(\Gamma f + \Gamma n)$. Center: survival probability multiplied by the slope of the complete fusion excitation function. Right: same distribution simulating experimental conditions: data taken at 1.5 MeV intervals with a target thickness covering 3 MeV; the thin line is a Gaussian fit.

Table 1. Difference (Experimental mass − Calculated mass) averaged on A, for Z from 102 to 108, and averaged on A and Z (last column) in 7 mass tables. The full list of DM(A, Z) with the 13 isotopes may be obtained from the author.

$Z =$	102	103	104	106	108	**Aver.**
Isotopes	6	2	2	2	1	
Mye94 [15]	−0.35	−0.50	−0.45	−0.55	−0.67	**−0.45**
Moe95 [5]	0.37	0.15	0.60	0.70	0.88	**0.46**
Abo95 [16]	−1.42	−1.21	−1.78	−1.18	−0.90	**−1.36**
Kou00 [17]	−1.11	−1.21	−1.32	−1.54	−1.60	**−1.26**
Lir01 [18]	0.15	0.20	0.14	0.07	0.17	**0.15**
Gor01 [19]	−0.68	−0.66	−1.09	−0.95	0.21	**−0.71**
Mun02 [20]	0.08	0.18	0.01	0.08	−0.08	**0.07**

as expected: 4.5 MeV. This value is close to FWHM values observed with the same target thickness [3].

3 Mass tables

Experiments determine 1n and 2n excitation functions in the center-of-mass system. The reaction Q value is subtracted to obtain E^*. It depends on the projectile and target masses, which are known, and on the compound nucleus mass, found in mass tables. Mass tables predictions differ by up to a few MeV. $E^*_{\rm max}$(1n) and Bf(CN−1n) values would differ by this same amount. A comparison of the mass tables to known mass values made it possible to reduce this uncertainty. For the 13 masses experimentally known for $Z \geq 102$, the differences between measured and calculated values, DM(A, Z), were listed. They were found to be *systematically* either negative [15–17,19], or positive [5,18,20].

Moreover, in each table DM(A, Z) do not exhibit a significant variation as a function of A. Therefore table 1 shows the average difference as a function of Z, $\langle {\rm DM}(Z)\rangle$, for the mass tables listed in chronological order. Two tables exhibit a very small difference: [18,20]. The reason is that these tables give mass values for nuclei with $Z \geq 82$ and the parameters in the formulas were fitted on data for these very heavy nuclei only. Therefore the 13 isotopes with $Z \geq 102$ have a much heavier weight in the fitting process than in mass tables using data from the whole mass range. However, the small differences observed from $Z = 102$ to 108 do not necessarily mean that the extrapolation to heavier Z's is closer to reality, so all mass tables were equally considered. As seen in table 1, in all cases no significant variation *versus* Z is observed. Therefore the average value, $\langle {\rm DM}(A, Z)\rangle$, in the last column, was used. It varies from −1.36 to +0.46 MeV. *Adjusted masses* for super-heavy nuclei in each table were then obtained by adding $\langle {\rm DM}(A, Z)\rangle$ of this table. These adjusted masses are much closer to each other. The uncertainties on E^* and Bf values due to the remaining differences are listed in fig. 3.

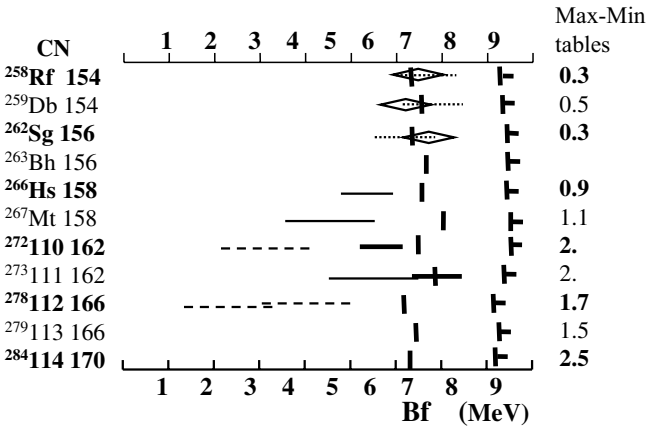

Fig. 3. Fission barrier values obtained for 1n (lines) and 2n (diamonds) evaporation residues from the compound nuclei listed at left. Diamonds and thin lines: from GSI data [3]; thick lines: from RIKEN data [4]. Dotted lines at $Z = 104$–106 show lower limits for the 1n ER (see text). Dashed lines for $Z = 110$ and 112 indicate very low statistics. Vertical mark: Sn(CN−1n); vertical+horizontal mark: Sn(CN−2n). "Max-Min tables": maximum difference due to different adjusted mass tables.

4 Extraction of fission barrier heights

For each reaction, the 1n excitation function was simulated as described above. Sn(CN), Sn(CN−1n) and

Sn(CN−2n) were taken as the average values of the different mass tables and are shown in fig. 3. In the third step, the excitation energies and energy widths of each simulated point were the same as in the actual data. Bf(CN−1n) was fitted to get agreement between simulated and measured $E^*_{\rm max}$(1n) values.

Figure 3 exhibits the results obtained by this method. The width of each symbol represents the estimated uncertainty due to experimental data.

When Sn(CN−1n) is close to Bf(CN−1n), it is difficult to know which one is responsible for the location of $E^*_{\rm max}$(1n). For $Z = 104$–106, values obtained from the 1n analysis (dotted line triangles in fig. 3) are indeed very close to Sn(CN−1n) values ($\sim$ 6.3 MeV for these odd-N nuclei) and it cannot be determined whether the maximum of 1n corresponds to Bf(CN−1n) or Sn(CN−1n). Then the same method was applied to 2n excitation functions. They offer two advantages: i) since the incident energy which corresponds to $E^*_{\rm max}$(2n) is close to $V_{\rm B}$, the peak shift due to the slope of the fusion cross-section, DE2, is small; ii) since these residues are even-N nuclei, Sn(CN−2n) is $\geq$ 8 MeV and Bf(CN−2n) can be measured up to this value. Bf(CN−2n) values are found to be $\sim$ 6.4 MeV for $Z = 104$–106 (diamonds in fig. 3).

For $Z \geq 108$, Bf values are obtained for 1n residues and are smaller than 6 MeV, which is consistent with the vanishing of 2n cross-sections relative to 1n. (This is also due to a much smaller reduction of the 1n cross-section than at smaller Z's, because the incident energy for 1n becomes close to, or larger than, $V_{\rm B}$.)

For $Z = 110$ and 111, different $E^*_{\rm max}$(1n) values were obtained at GSI and RIKEN [3,4]. The beam energies have to be exactly known. For $Z = 112$, the two dashed line triangles are indicative only since they come from 1 event only at each of two incident energies [3].

Remark: in fission barrier tables [5,9,10], fig. 1 shows that the differences between neighboring isotopes are smaller than the experimental uncertainties in fig. 3. The present data are then unable to check odd-even N effects on Bf.

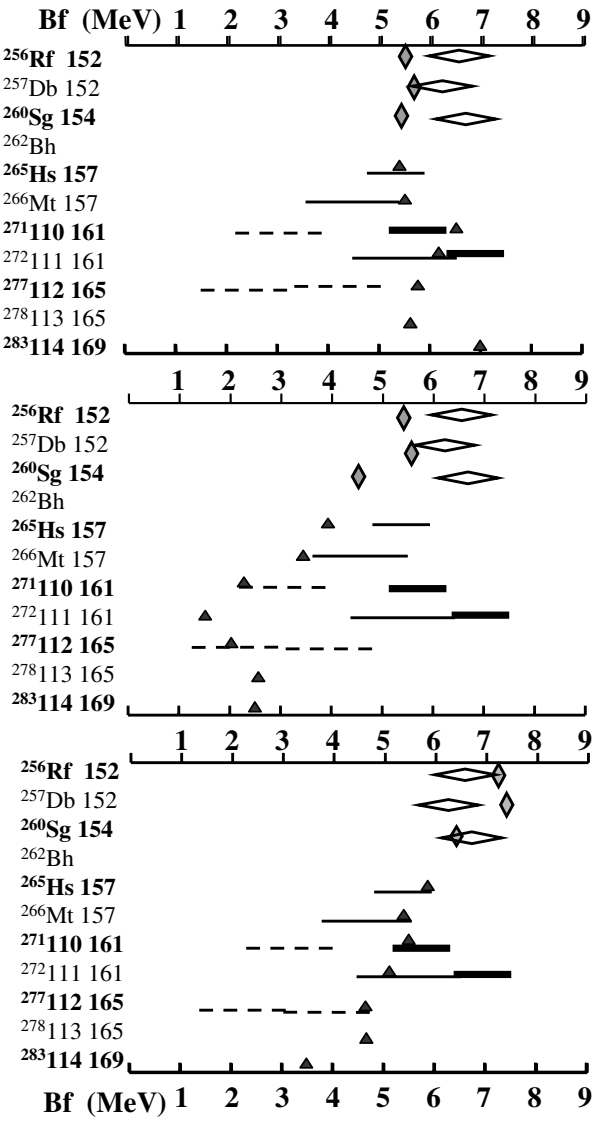

Fig. 4. Fission barrier values obtained for 1n (lines) and 2n (diamonds) evaporation residues listed at left and compared to 3 theoretical fission barrier tables. Diamonds and thin lines: from GSI data [3]; thick lines: from RIKEN data [4]. Solid small symbols: theoretical values. Top: Moeller *et al.* [5]. Middle: Mamdouh *et al.* [9]. Bottom: Muntian *et al.* [10].

5 Conclusion

These fission barrier values are not accurate. Nevertheless, they may be compared to fission barrier theoretical predictions [5,9,10]. This comparison is made in fig. 4. Mamdouh *et al.* [9] give values which are systematically smaller than the data, by 2 to 3 MeV. Moeller shell correction at ground state [5] plus liquid-drop correction at saddle [6] predicts a rather constant value, 5–6 MeV, for the nuclei studied here; it slightly underestimates the data for $Z = 104$ and 105 and is in agreement, within experimental uncertainties, for $Z \geq 108$. An overall rough agreement is observed with Muntian *et al.* table [10]. It has to be confirmed by more accurate data on $Z = 110$–112. Remark: its predicted values for the compound nucleus and the 1n evaporation residue ^{283}114 formed in cold fusion of the system ^{76}Ge + ^{208}Pb are smaller than 4 MeV; this would decrease very much the survival probability and the 1n cross-section.

Another comparison can be made with the Bf lower limits of heavier elements and isotopes mentioned at the beginning of this paper [2]. For $^{283-286}$112, $^{288-292}$114 and $^{292-296}$116 isotopes, they are 5.5, 6.7 and 6.4 MeV, respectively. These lower limits are larger than the values predicted by Muntian *et al.*: 3.5–4.1, 4.5–5.8 and 5.4–6.5 MeV, respectively. They are smaller than (and therefore do not contradict) the values predicted by Moeller *et al.*: 6.2–6.6, 8.1–8.9 and 8.3–9 MeV, respectively, and by Mamdouh *et al.*: 7.1–6.5, 6.1–7.3 and 6.5–7.6 MeV, respectively.

With these two sets of inaccurate data, the predictions which have the best overall agreement are those from Moeller *et al.* However, more data, and more accurate ones, on fission barrier heights of super-heavy nuclei have to be obtained in order to be able to reach a firm conclusion.

The author expresses his deep thanks to S. Hofmann and K. Morita and their colleagues for detailed information on their data, to Y. Abe, Y. Aritomo, G. Giardina, M. Ohta, A. Sobiczewski, W.J. Swiatecki and V.I. Zagrebaev for communication of results prior publication, and to all of them and S. Grévy for fruitful discussions.

References

1. M.G. Itkis *et al.*, *Proceedings on Fusion Dynamics at the Extremes, Dubna, Russia, 2000*, edited by Y. Oganessian, V. Zagrebaev (World Scientific, 2001).
2. M.G. Itkis *et al.*, Phys. Rev. C **65**, 044602 (2002).
3. S. Hofmann, G. Münzenberg, Rev. Mod. Phys. **72**, 733 (2000) and private communication.
4. K. Morita *et al.*, Riken Accel. Prog. Rep. **36**, 204 (2003), and private communication.
5. P. Möller, J.R. Nix, W.D. Myers, W.J. Swiatecki, At. Data Nucl. Data Tables **59**, 185 (1995)
6. Y. Aritomo, private communication.
7. W.J. Swiatecki, K. Siwek-Wilczynska, J. Wilczynski, Acta Phys. Pol. B **34**, 2049 (2003).
8. G. Giardina *et al.*, Eur. Phys. J. A. **8**, 205 (2000) and private communication.
9. A. Mamdouh, J.M. Pearson, M. Rayet, F. Tondeur, Nucl. Phys. A **679**, 337 (2001).
10. I. Muntian, Z. Patyk, A. Sobiczewski, Acta Phys. Pol. B **34**, 2141 (2003).
11. J. Péter *et al.*, *Proceedings of the International Symposium EXON, Baikal, Russia*, edited by Yu. Penionzhkevic, E. Cherepanov (World Scientific, 2002) p. 41.
12. M.G. Itkis *et al.*, Nuovo Cimento A **111**, 783 (1998).
13. Y. Aritomo, M. Ohta, *Proceedings on Fusion Dynamics at the Extremes, Dubna, Russia, 2000*, edited by Y. Oganessian, V. Zagrebaev (World Scientific, 2001) and private communication.
14. B. Bouriquet, Y. Abe, D. Boilley, preprint (2003) and private communication.
15. W.D. Myers, W.J. Swiatecki, Nucl. Phys A **601**, 141 (1996) and report LBL-36803 (1994).
16. Y. Aboussir, J.M. Pearson, A.K. Dutta, F. Tondeur, At. Data Nucl. Data Tables **61**, 127 (1995); M. Rayet, private communication.
17. H. Koura, M. Uno, T. Tachibana, M. Yamada Nucl. Phys. A **674**, 47 (2000).
18. S. Liran, A. Marinov, N. Zeldes, Phys. Rev C **62**, 047301 (2001).
19. S. Goriely, F. Tondeur, J.M. Pearson, At. Data Nucl. Data Tables **77**, 311 (2001).
20. I. Muntian, Z. Patyk, A. Sobiczewski, Yad. Fiz. (Phys. At. Nucl.) **66**, 1015 (2003).